Available online at www.sciencedirect.com

ScienceDirect

International Journal of Heat and Mass Transfer 50 (2007) 702–712

International Journal of HEAT and MASS TRANSFER

www.elsevier.com/locate/ijhmt

Entropy flow and generation in radiative transfer between surfaces

Z.M. Zhang *, S. Basu

George W. Woodruff School of Mechanical Engineering, Georgia Institute of Technolgy, Atlanta, GA 30332, USA

Received 9 November 2005; received in revised form 29 June 2006
Available online 22 September 2006

Abstract

Entropy of radiation has been used to derive the laws of blackbody radiation and determine the maximum efficiency of solar energy conversion. Along with the advancement in thermophotovoltaic technologies and nanoscale heat radiation, there is an urgent need to determine the entropy flow and generation in radiative transfer between nonideal surfaces when multiple reflections are significant. This paper investigates entropy flow and generation when incoherent multiple reflections are included, without considering the effects of interference and photon tunneling. The concept of partial equilibrium is applied to interpret the *monochromatic radiation temperature* of thermal radiation, $T_\lambda(\lambda,\Omega)$, which is dependent on both wavelength λ and direction Ω. The entropy flux and generation can thus be evaluated for nonideal surfaces. It is shown that several approximate expressions found in the literature can result in significant errors in entropy analysis even for diffuse-gray surfaces. The present study advances the thermodynamics of nonequilibrium thermal radiation and will have a significant impact on the future development of thermophotovoltaic and other radiative energy conversion devices.

Keywords: Entropy; Equilibrium; Photon; Thermal radiation; Thermodynamics

1. Introduction

Thermal radiation is the dominant mode of heat transfer in direct solar energy conversion (photovoltaic devices) as well as in thermophotovoltaic cells, which can employ combustion as the high-temperature source [1]. Radiative heat transfer can be enhanced by orders of magnitude and may be applied to increase energy conversion efficiency [2,3]. Nanostructures offer new opportunities for engineering the surface properties to improve the conversion efficiency from a heated body to electrical power [4]. The attainable efficiency in energy conversion systems depends on the success of minimizing the entropy generation [5].

The concept of entropy of radiation has played an essential role in development of the theory of blackbody radiation. Boltzmann in 1884 investigated the thermodynamics of radiation in an isothermal enclosure and proved the empirical equation $e_b(T) = \sigma T^4$ obtained by Stefan for the blackbody emissive power. Here, T is the temperature of the blackbody and σ is the Stefan–Boltzmann constant. In doing so, he also determined the associated entropy flux to be $s_b(T) = \frac{4}{3}\sigma T^3$. After introducing the radiation quanta, Planck expressed the spectral entropy associated with each vibrational frequency mode and formulated the famous law of blackbody radiation in 1900 [6]. Beretta and Gyftopoulos [7] pointed out that electromagnetic radiation carries both energy and entropy and is neither work nor heat interaction. Saying in other words, for blackbody radiative transfer between two systems at different temperatures, the rate of entropy transfer is not equal to the ratio of energy transfer rate between the two systems to the temperature of either of the systems. Modeling laser beam as an incoherent source and using the definition of spectral radiation entropy, Essex et al. [8] calculated the temperature of the near monochromatic laser radiation from a 1 mW He–Ne laser at 632.8 nm wavelength to be as high as 10^{10} K. Laser energy is considered as (almost) equivalent to work with very low entropy and a very high radiation temperature.

* Corresponding author. Tel.: +1 404 385 4225; fax: +1 404 894 8496.
E-mail address: zhuomin.zhang@me.gatech.edu (Z.M. Zhang).

0017-9310/$ - see front matter © 2006 Elsevier Ltd. All rights reserved.
doi:10.1016/j.ijheatmasstransfer.2006.07.009

Nomenclature

Glossary

c	speed of light in vacuum, 2.998×10^8 m/s
e	emissive power, W/m^2
h	Planck's constant, 6.626×10^{-34} J s
I	intensity, W/m^2 sr
k_B	Boltzmann's constant, 1.381×10^{-23} J/K
L	radiation entropy intensity, W/K m^2
n	refractive index
$\hat{\mathbf{n}}$	surface normal
q	heat flux, W/m^2
S	entropy of the system per unit surface area, J/K m^2
s	entropy flux, W/K m^2
s_g	entropy generation rate per unit surface area, W/K m^2
T	temperature, K
T_λ	monochromatic radiation temperature, K
U	internal energy of the system per unit surface area, J/m^2

Greek symbols

β	polarization parameter: $\beta = 1$ linearly polarized; $\beta = 2$ unpolarized
ε	emissivity
θ	zenith angle, deg
λ	wavelength, m
σ	the Stefan–Boltzmann constant, 5.670×10^{-8} W/m^2 K^4
ϕ	azimuthal angle, deg
Ω	solid angle, sr, also as the unit vector in the direction of propagation

Subscripts

1 or 2	surface 1 or 2
abs	absorbed
b	blackbody
cond	conduction
emit	emitted
in	incoming
out	outgoing
ref	reflected
λ	spectral property

Superscripts

+	forward
−	backward

Petela [9] realized the importance of entropy and exergy of radiation to energy conversion in the 1960s. While the spectral nature of thermal radiation was recognized, he introduced a simplified formula, without spectral integration, for the total entropy leaving a diffuse-gray surface as $\varepsilon s_b(T_1)$, where ε is the emissivity and T_1 is the temperature of the emitting surface. Even for a free emitting surface, such an expression may result in a large error when the emissivity is small. In one of his recent papers on this subject, Petela [10] further assumed that the absorbed entropy of such a surface for radiation coming from a blackbody at temperature T_2 to be $\varepsilon s_b(T_2)$, which is also an oversimplification as will be shown later. In the 1980s, extensive studies were published to determine the maximum efficiency of solar energy converters [11–13]. These studies generally dealt with blackbody radiation and did not concern the spectral properties of radiation; see Bejan's text for a comprehensive review and discussion of this subject [13]. Arpaci [14] modeled radiation entropy generation for turbulent flow and heat transfer. His analysis was limited to optically thick cases when the radiative transfer equation is reduced to a diffusion equation similar to heat conduction.

Landsberg and Tonge [15] introduced the concept of *dilute blackbody radiation* and an *effective temperature*. They also proposed other temperature-related definitions such as the *flux temperature*, in addition to the *brightness temperature* [16]. However, they did not apply their theory for multiple reflections. Furthermore, the repeated usage of various definitions of temperature is confusing and prevents the general acceptance of their methodology. Wright et al. [17] obtained approximate expressions for calculating the entropy of radiation emitted from a gray body without considering reflection. Whale [18] drew an analogy between far-field radiation and near-field radiation using the concept of flux temperature but further research is needed to assess the validity of simply extending the far-field theory to the near-field situation. Caldas and Semiao [19] recently extended the formulation of radiation entropy to participating media and numerically determined the entropy generation during radiative transfer. However, the entropy generation at the wall that could be important for their studied systems was not included in their analysis and numerical simulation. Similar analysis was performed by Liu and Chu [20] considering a participating medium between blackbody walls.

In the present work, attention is paid to the entropy associated with the emission, transmission, and reflection processes of thermal radiation by a surface, which is opaque or semi-infinite, or a semitransparent slab. Furthermore, the entropy generation during radiative transfer between two isothermal diffuse-gray surfaces is analyzed, considering the entropy components associated with absorption, emission, and reflection of radiation.

2. Theoretical background

For a blackbody enclosure at thermal equilibrium, one can use a cylinder-piston arrangement to perform a thermodynamic analysis that will lead to the Stefan–Boltzmann law, and expressions for the entropy, pressure, and specific heat of blackbody radiation in terms of its temperature [21,22]. For blackbody radiation in vacuum, the spectral distributions of the emissive power and intensity are given by Planck's law,

$$e_{\lambda,\mathrm{b}}(\lambda,T)=\pi I_{\lambda,\mathrm{b}}(\lambda,T)=\frac{\beta\pi hc^2}{\lambda^5(\mathrm{e}^{hc/k_\mathrm{B}\lambda T}-1)} \quad (1)$$

where c is speed of light in vacuum, h is Planck's constant, and k_B is Boltzmann's constant. Here, β is a polarization parameter in such a way that $\beta=1$ is for either the transverse electric (TE) wave or the transverse magnetic (TM) wave, and $\beta=2$ is for unpolarized radiation. It is noticed that the intensity of blackbody radiation is independent of direction. The *radiation entropy intensity* can be expressed in terms of the (energy) intensity as follows [22]:

$$L_\lambda(I_\lambda)=\frac{\beta k_\mathrm{B}c}{\lambda^4}\left[\left(1+\frac{\lambda^5 I_\lambda}{\beta hc^2}\right)\ln\left(1+\frac{\lambda^5 I_\lambda}{\beta hc^2}\right)-\frac{\lambda^5 I_\lambda}{\beta hc^2}\ln\left(\frac{\lambda^5 I_\lambda}{\beta hc^2}\right)\right] \quad (2)$$

The radiation entropy flux is calculated by integrating the radiation entropy intensity, that is,

$$s_\lambda=\int_{\phi=0}^{2\pi}\int_{\theta=0}^{\pi/2}L_\lambda\cos\theta\sin\theta\,\mathrm{d}\theta\,\mathrm{d}\phi \quad (3)$$

For a blackbody or diffuse radiation, we have $s_\lambda=\pi L_\lambda$. In a closed enclosure with a volume V, the temperature of the system is defined as $\frac{1}{T}=\left(\frac{\partial S}{\partial U}\right)_V$, where S and U refer to the entropy and internal energy of the system, respectively [23]. The *monochromatic radiation temperature*, or simply as either the *monochromatic temperature* or *radiation temperature*, can be defined based on the spectral intensities (since they are proportional to the energy and entropy densities of the electromagnetic radiation), viz.

$$\frac{1}{T_\lambda(\lambda,\Omega)}=\frac{\partial L_\lambda}{\partial I_\lambda} \quad (4)$$

At thermodynamic equilibrium, it is obvious that the above expression gives the physical temperature of the photon gas regardless of the radiative properties of the wall, as long as the location is not too close to the surface of the wall where near-field radiation dominates. One can rewrite Eq. (4) using Eq. (2) as follows:

$$T_\lambda(I_\lambda)=\frac{hc/\lambda k_\mathrm{B}}{\ln\left(\frac{\beta hc^2}{\lambda^5 I_\lambda}+1\right)} \quad (5)$$

Consider a nearly monochromatic laser beam from a pointer, the intensity I_λ can easily be calculated based on its power, wavelength interval, beam diameter, and divergence. Assuming that the light is polarized and can be treated as in an equilibrium state, the entropy intensity L_λ can be calculated from Eq. (2) and, similarly, the "temperature" of the laser light can be obtained by either Eq. (4) or (5). It can be easily shown that this temperature is the one that corresponds to a blackbody radiation spectrum with the same intensity at the laser wavelength. Such a temperature is often called the brightness temperature or *radiance temperature*, in optical pyrometry and radiation thermometry [24] as an equivalent temperature that a blackbody would have in order for it to emit the same intensity. The entropy defined in Eq. (2) is generally applicable for incoherent radiation, as can be proved by nonequilibrium thermodynamics [25]. Furthermore, the temperature defined in Eq. (4) is a thermodynamic temperature for the monochromatic or spectral-directional radiation [16]. As pointed out by Caldas and Semiao [19], there exist *infinite* radiation temperatures at any spatial location for steady-state thermal radiation in an enclosure that is not at thermal equilibrium. An immediate paradox is as follows. If a surface, whose emissivity is not equal to 1, is placed inside a blackbody enclosure, what is the temperature of the emitted, reflected, and absorbed radiation? The solution is that one should substitute the *combined intensity*, rather than the reflected intensity or emitted intensity, into Eq. (2) to evaluate the entropy and into Eq. (5) to evaluate the temperature. Because the enclosure is at thermal equilibrium, the combined intensity is independent of the surface properties and wavelength. The obtained monochromatic temperature based on the combined intensity will always be the equilibrium temperature of the enclosure. Multiple reflections can be treated in the same way by using their combined intensity to define the radiation temperature. Entropy production can occur in radiation without the generation of heat. If a nearly collimated radiation is diffusely scattered by a perfectly reflecting (rough) surface, the scattered radiation will have a much lower intensity due to the expanded solid angle. The process is accompanied by entropy increase and hence is irreversible. On the other hand, if a nearly collimated light is split into two beams using a beam splitter, the transmitted and reflected beams can interfere with each other and the original intensity can be realized again after another beam splitter in the Mach–Zehnder interferometer. This process may be reversible because the two beams are correlated [26]. The correlated or coherent beams have lower entropy than those with the same intensity at thermodynamic equilibrium. The concept of monochromatic temperature is applicable only if the maximum entropy has been obtained. The calculation of radiation entropy based on Eq. (2) relies on the following three hypotheses:

1. For either a vacuum or a participating medium, the intensities of radiation at any given location can be superimposed regardless of where they originate, as long as all the rays fall within the same infinitesimal solid angle (pencil cone) and spectral interval (either based on the wavelength or frequency). The resulting intensity is called the combined intensity. Note that the intensity cannot be a simple addition in the presence of strong interference and diffraction. In essence, wave interference and diffraction effects are neglected, and the radia-

tion field is treated as incoherent under this hypothesis. Furthermore, if a participating medium is present, it is assumed nondispersive so that the group velocity and the phase velocity of electromagnetic waves are the same and independent of the frequency.

2. The monochromatic radiation temperature can be calculated based on Eq. (5) using the combined intensity. Radiation temperature is in general dependant on the wavelength or frequency, direction, and polarization. Photons are relativistic quanta that behave very differently from molecules or electrons. Photon travels with the same speed and do not collide with each other. The interaction between photons is a wave effect that has been excluded in the first hypothesis. Hence, photons of different frequencies can coexist in the same volume element but with different radiation temperatures. In addition, photons in different directions can have different monochromatic temperatures even with the same frequency. In the case when the radiation consists of two linear polarizations with different intensities, the monochromatic temperatures will be different for different polarizations. In essence, nonequilibrium radiation may be regarded as in a partial equilibrium state, so that each subsystem with its own wavelength, direction, and polarization can be considered as in an equilibrium state that is independent of others. A detailed discussion about partial thermodynamic equilibrium can be found from [23]. It should also be noted that if the medium is optically thick, local equilibrium will be established; in which case the radiation temperature reduces to the local temperature of the medium.
3. The entropy intensity is defined based on the combined intensity according to Eq. (2). The sum of the entropies of all individual rays should be calculated based on the radiation temperature of the combined intensity. Because both energy and entropy are additive, the ratio of the entropy intensity of each ray to the entropy intensity of the combined radiation is equal to the ratio of the (energy) intensity of that ray to the combined intensity. This hypothesis allows evaluation of the absorbed, emitted, and reflected entropy at individual surfaces.

The logical interpretation of radiation temperature and radiation entropy allows a thermodynamic analysis of radiative heat transfer in various situations. The present study focuses on the radiative transfer between surfaces. The energy and entropy equations for a plate at temperature T_1 whose surface emissivity is ε_1 can be derived with the help of Fig. 1. The elemental solid angle is $\mathrm{d}\Omega$, and its direction is indicated by Ω, which is determined by the zenith angle θ from surface normal $\hat{\mathbf{n}}$ and the azimuthal angle ϕ. It is assumed that radiation is absorbed or emitted from a very thin skin layer.

The energy balance of the control volume per unit surface area can be written as

$$\dot{U} = q_{\text{in}} - q_{\text{out}} + q_{\text{cond}} \tag{6}$$

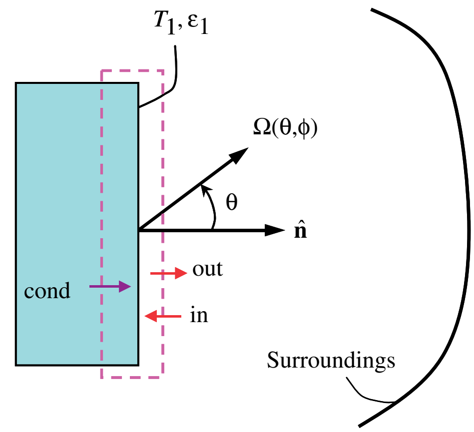

Fig. 1. Energy and entropy balance for radiative heat transfer at the surface of a plate.

where $\dot{U}$ is the rate of internal energy change in the control volume, q_{in} and q_{out} are the incoming and outgoing radiative heat flux (or energy flux to be more precise), and q_{cond} is the conduction heat flux entering the left side of the control volume. Hemispherical and spectral integration of the intensity gives the heat fluxes:

$$q_{\text{in}} = \int_{\lambda=0}^{\infty} \mathrm{d}\lambda \int_{\hat{\mathbf{n}}\cdot\Omega<0} I_\lambda(\lambda,\Omega)\hat{\mathbf{n}}\cdot\Omega\,\mathrm{d}\Omega \tag{7a}$$

and

$$q_{\text{out}} = \int_{\lambda=0}^{\infty} \mathrm{d}\lambda \int_{\hat{\mathbf{n}}\cdot\Omega>0} I_\lambda(\lambda,\Omega)\hat{\mathbf{n}}\cdot\Omega\,\mathrm{d}\Omega \tag{7b}$$

For the outgoing radiation, the intensity is the sum of the emitted and the reflected intensities. These equations have been studied extensively in radiative transfer texts [21,27] and will not be repeated here. The next step is to express the entropy balance as follows [13,23]:

$$\dot{S} = s_{\text{in}} - s_{\text{out}} + s_{\text{cond}} + s_{\text{g}} \tag{8}$$

All quantities expressed above are for unit time and unit area, and the subscripts have the same meaning as in Eq. (6), except that "g" stands for generation. Eq. (8) states that the change of entropy in the control volume is equal to the net entropy received by the control volume plus entropy generation. Similar to the heat fluxes, the entropy fluxes can be calculated by

$$s_{\text{in}} = \int_0^{\infty} \mathrm{d}\lambda \int_{\hat{\mathbf{n}}\cdot\Omega<0} L_\lambda(\lambda,\Omega)\hat{\mathbf{n}}\cdot\Omega\,\mathrm{d}\Omega \tag{9a}$$

and

$$s_{\text{out}} = \int_0^{\infty} \mathrm{d}\lambda \int_{\hat{\mathbf{n}}\cdot\Omega>0} L_\lambda(\lambda,\Omega)\hat{\mathbf{n}}\cdot\Omega\,\mathrm{d}\Omega \tag{9b}$$

where L_λ is determined from I_λ by Eq. (2). Because the plate is maintained at a constant temperature, assuming the thermal conductivity is very high, $s_{\text{cond}} = q_{\text{cond}}/T_1$. The left-hand sides in Eqs. (6) and (8) are zero at the steady state. Therefore, Eq. (9) can be recast to evaluate the entropy generation rate per unit surface areas due to radiative heat transfer in the following:

$$s_g = \frac{q_{in} - q_{out}}{T_1} - (s_{in} - s_{out}) \tag{10}$$

Similar to radiative heat transfer analysis [27], entropy flow towards a surface and away from a surface can be characterized by an incoming component and an outgoing component. Can one separate the emitted entropy from the reflected entropy? Yes. This can be done by first separating the outgoing intensity into an emitted component, which is the emissivity multiplied by the blackbody emissive power, and a reflected component, which depends on the incident spectral intensity and the bidirectional reflectance of the surface [28]. The ratio of the emitted intensity to the combined intensity is a function of the wavelength and direction, given by

$$X(\lambda, \Omega) = \varepsilon_1 I_{\lambda,b}(\lambda, T)/I_\lambda, \quad \text{for } \Omega \cdot \hat{\mathbf{n}} > 0 \text{ only} \tag{11}$$

where the function X is the fraction of the emitted intensity, and ε_1 in general is dependent on the wavelength and direction as well. The emitted entropy can be calculated by

$$L_{\lambda,emit}(\lambda, \Omega) = X(\lambda, \Omega) L_\lambda(I_\lambda) \tag{12}$$

Notice again that the combined entropy intensity L_λ is evaluated from the combined intensity I_λ by Eq. (2). The proportionality used in Eqs. (11) and (12) is based on the concept of partial equilibrium or spectral-directional equilibrium of thermal radiation as outlined in the second hypothesis given above. In an equilibrium state, if the number of particles is divided by two, the energy and entropy are also equally divided because both are extensive properties. The emitted entropy flux, s_{emit}, can be obtained by substituting $L_{\lambda,emit}(\lambda, \Omega)$ for $L_\lambda(\lambda, \Omega)$ in Eq. (9b) and then performing the integration. The reflected entropy flux becomes $s_{ref} = s_{out} - s_{emit}$, and the absorbed entropy flux is thus $s_{abs} = s_{in} - s_{ref} = s_{in} - s_{out} + s_{emit}$.

The physical interpretation of the entropy of emission is the entropy associated with the photons that are emitted by the surface (only spontaneous emission is considered here). The radiative energy emitted by the surface depends only on its temperature and emissivity, independent of the environment. On the contrary, the emitted entropy is dependent on the incoming radiation, if the incoming radiation from the surrounding cannot be neglected. The reason is that the monochromatic temperature of emission is affected by the incoming photons. For the same amount of photon flux, the entropy of free emission, i.e., $X(\lambda, \Omega) = 1$, is different from the entropy of emission when the incoming intensity is nonzero. Applications of the analytic methodology developed here will be described in the next section.

3. Entropy analysis applied to special cases

Several special cases are chosen to illustrate the entropy formulation in radiative heat transfer. The first case is for *free emission* from a diffuse-gray body. Here, free emission means that the surface is enclosed in an empty space with large surroundings at zero absolute temperature. The second case is for free emission from a semi-infinite medium with a refractive index that is independent of wavelength. Therefore, the surface is gray but not diffuse and there is an effect of polarization on the emission. The third case is the entropy generated upon reflection and transmission through a semitransparent slab of given refractive index. The effects of polarization and multiple reflections are considered, but interference and absorption are neglected. Semitransparent windows are extensively used in solar energy applications, including solar collectors and buildings. The fourth case is the radiative transfer between two infinite parallel plates at different temperatures separated by vacuum. Both the plates are modeled as diffuse-gray and opaque with different emissivities. The separation distance is assumed to be large enough so that interference and evanescent wave effects can be neglected. At steady state, partial radiation equilibrium is established inside such a cavity but the radiation temperature depends on both the wavelength and direction. The entropy generation due to the emission, reflection, and absorption of thermal radiation is analyzed for each surface.

3.1. Free emission from a diffuse-gray surface

The simplest case besides blackbody emission is a diffuse-gray surface emitting towards a large, cold environment. There is no absorption and no incoming fluxes, and from the definition of emissivity, the outgoing or emitted heat flux is

$$q_{emit} = \varepsilon \sigma T^4 \tag{13}$$

where ε and T are the emissivity and temperature of the surface (the subscript 1 in Fig. 1 is omitted for simplicity). Intuitively, one would guess that, in analogy to the blackbody emission with an emissive power $e_b = \sigma T^4$ and entropy flux of $s_b = \frac{4}{3}\sigma T^3$, the total emitted entropy flux of the diffuse-gray surface could be given by

$$s_{emit} = \varepsilon \frac{4}{3} \sigma T^3 \tag{14}$$

This is Eq. (7) in the 1964 paper by Petela [9]. After some 40 years, the same equation was used in his 2003 paper for gray surfaces, see Eq. (29) in Ref. [10]. If Eq. (14) holds, the entropy generation by free emission becomes

$$s_g = s_{emit} - \frac{q_{emit}}{T} = \frac{1}{3}\varepsilon \sigma T^3 \tag{15}$$

which is Eq. (30) in Ref. [10]. Fig. 2 shows the calculation results according to Eq. (9b), which is called the exact solution, and Petela's approximate expression, i.e., Eq. (14) in the present paper. The emitted entropy is normalized to the blackbody entropy. It can be seen from Fig. 2 that Eq. (14) is exact only when the emissivity is equal to one, as for the blackbody case. When the emissivity is less than unity, Eq. (14) always underpredicts the emitted entropy,

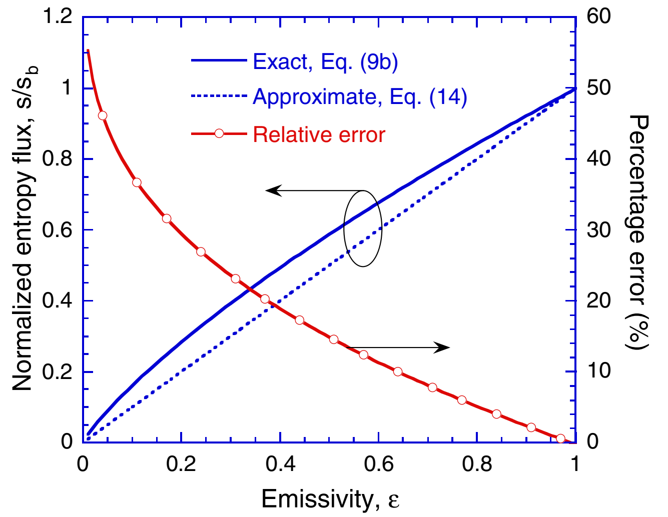

Fig. 2. Outgoing entropy flux, normalized to that of a blackbody, for a free emitting surface as a function of its emissivity. The percentage error of the approximation is shown on the right.

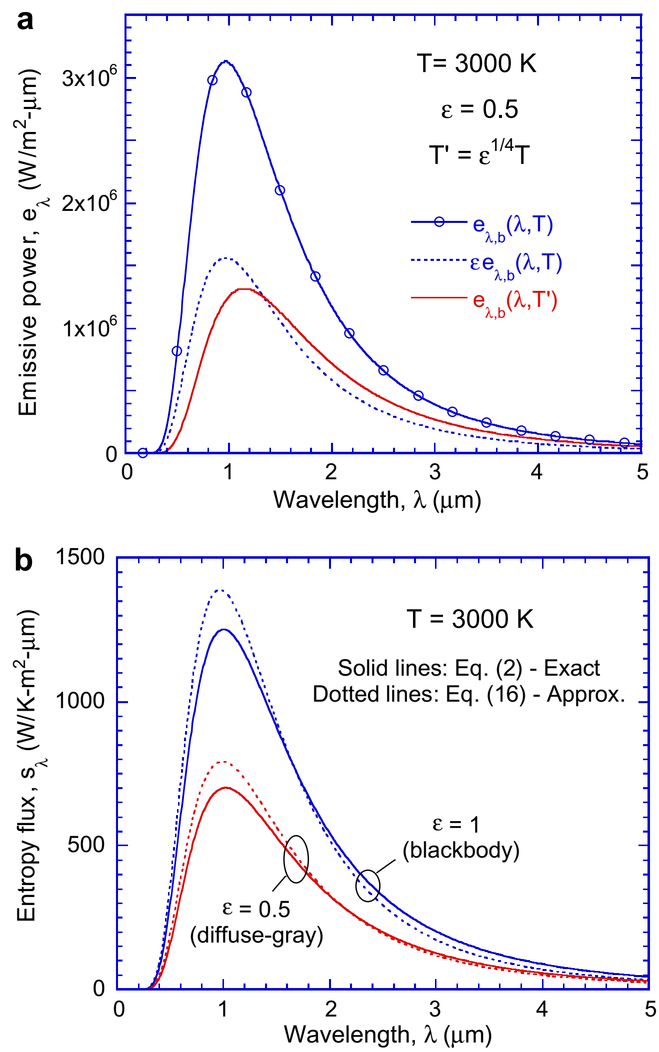

Fig. 3. Spectral distribution of (a) emissive power and (b) entropy flux.

and hence the entropy generation according to Eq. (15) is also erroneously underpredicted. The error caused by this approximation may be small if the source has a large emissivity value or is near a blackbody. Nevertheless, caution should be taken before applying Eq. (14) in analyzing the conversion efficiencies for nonideal surfaces. The reason why the total emissivity should not be directly used in the total entropy expression is the following. Consider a source temperature at 3000 K, the blackbody emissive power is the highest as shown in Fig. 3a. For a diffuse-gray surface with an emissivity of 0.5, the spectral distribution of the emissive power would be proportional to the blackbody emissive power at 3000 K. This curve, however, is not a blackbody distribution function. Suppose an equivalent temperature of the radiation based on the total emissive power is to be used. By setting $\sigma T'^4 = \varepsilon\sigma T^4$, one obtains $T' =$ 1681.8 K. The peak of the spectral distribution that corresponds to the blackbody distribution at T' will shift to a longer wavelength, as illustrated in Fig. 3a. Only at the crossover wavelength, which is approximately 1.33 μm, the monochromatic temperature of the diffuse-gray body is the same as T'. Saying in other words, the radiation temperature even for a gray body is wavelength dependent. The nonequilibrium nature of gray-surface emission was noticed by Landsberg and Tonge [15] and termed this type of radiation, dilute blackbody radiation. The present work uses very few new definitions, and links the entropy analysis directly to thermal radiation analysis for which the heat transfer community is already very familiar with.

Bejan arrived at an expression for the radiation entropy intensity:

$$L_\lambda = \frac{4I_\lambda}{3T_\lambda} \tag{16}$$

which is Eq. (9.47) in Ref. [13]. For radiation from a blackbody, the monochromatic temperature is not a function of wavelength; hence, the spectral integration of Eq. (16) yields $L = \frac{4}{3}\frac{\sigma T^3}{\pi}$, as expected. A direct comparison of the spectral distribution between the exact expression of L_λ given in Eq. (2) and the approximate expression of Eq. (16) is shown in Fig. 3b. It can be seen that the approximate expression overpredicts the entropy flux at shorter wavelengths and underpredicts the entropy flux at longer wavelengths, even for a blackbody source. Given the available computational capabilities nowadays, it is a relatively easy task to perform the integration using the spectral entropy distribution given in Eq. (2) to prevent the error associated with this approximation.

The radiation temperature is plotted against wavelength for diffuse-gray surfaces with different emissivities, as shown in Fig. 4. The radiation temperature is the same as the surface temperature for a blackbody and is independent of wavelength. As the emissivity is reduced, the monochromatic temperature decreases faster at longer wavelengths, i.e., in the Rayleigh–Jeans limit, where the blackbody emissive power is proportional to temperature. At very short wavelengths, the emissive power is a strong function of

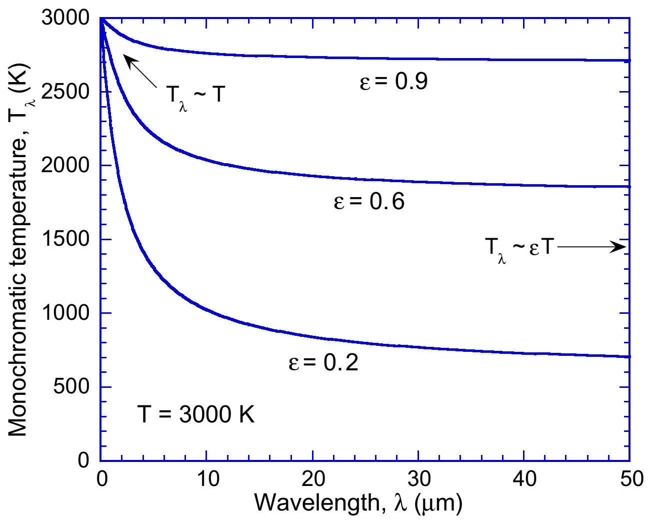

Fig. 4. Spectral distribution of the monochromatic temperature for free emitting surfaces at 3000 K with different emissivities.

temperature, and thus the effect of emissivity on the radiation temperature is very weak.

3.2. Free emission from a semi-infinite medium with refractive index n

For the purpose of illustrating the polarization effect, a semi-infinite medium with a refractive index n at a uniform temperature T is considered as the emission source. The emission is again towards free space. The emissivity for either TE or TM wave can be calculated based on Kirchhoff's law by subtracting the reflectivity calculated using Fresnel's equations [21]. The emitted intensity for each polarization is used to compute the entropy of emission and monochromatic temperature. The ratio of the monochromatic temperature to the medium temperature is shown in Fig. 5, along with the directional emissivity, for $n = 3$. Note that the temperature ratio depends on the product λT and $\lambda T = 3000$ μm K is near the peak wavelength in the emissive power given by Wien's displacement law and 99.5% of the radiative energy is within the spectral region from $\lambda T = 300$ μm K to $\lambda T = 30{,}000$ μm K. At the Brewster angle ($\theta_B = 71.57°$), where the emissivity is equal to 1, the monochromatic temperature is the same as the temperature of the medium. The effect of angular dependence and polarization is clearly demonstrated in Fig. 5. Note again that the effect of emissivity on the monochromatic temperature is larger towards longer wavelengths.

The normalized emitted entropy as a function of the refractive index is shown in Fig. 6, together with the hemispherical and normal emissivities. Note that a constant refractive index is assumed so that the emission is independent of the wavelength. For a gray surface, $s/s_b \neq f(T)$ as can be seen from Eqs. (2) and (9b). The hemispherical emissivity is obtained by integrating the average emissivity over the hemisphere. For the entropy calculation, individual emissivity is first multiplied by the blackbody intensity to

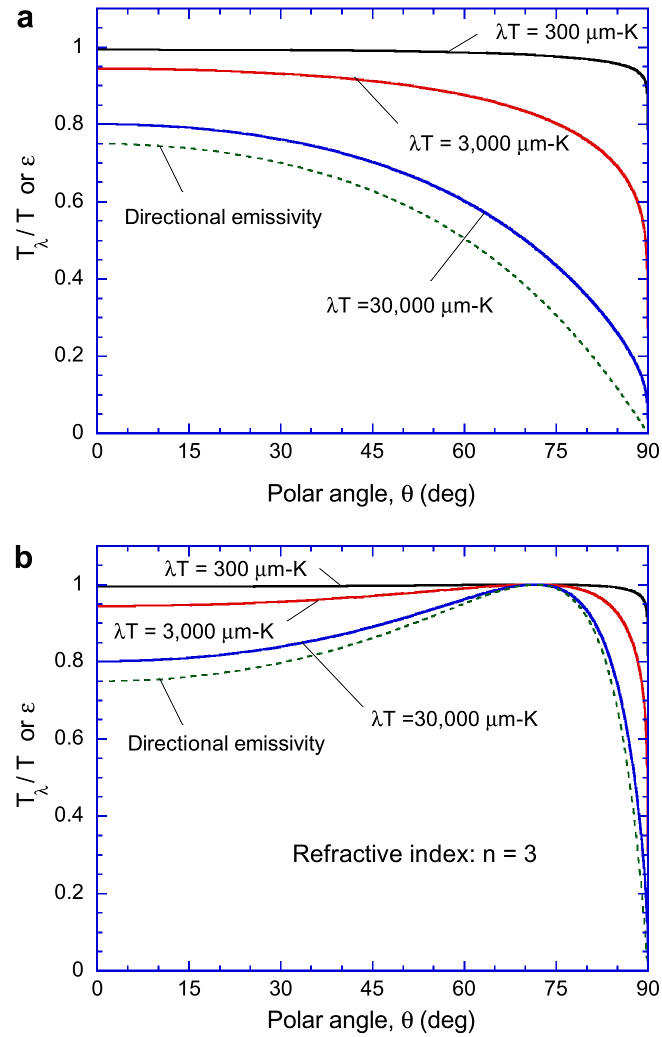

Fig. 5. Temperature ratio versus the polar angle for thermal emission from a semi-infinite medium with a refractive index $n = 3$, where the directional emissivity is also shown: (a) TE wave and (b) TM wave.

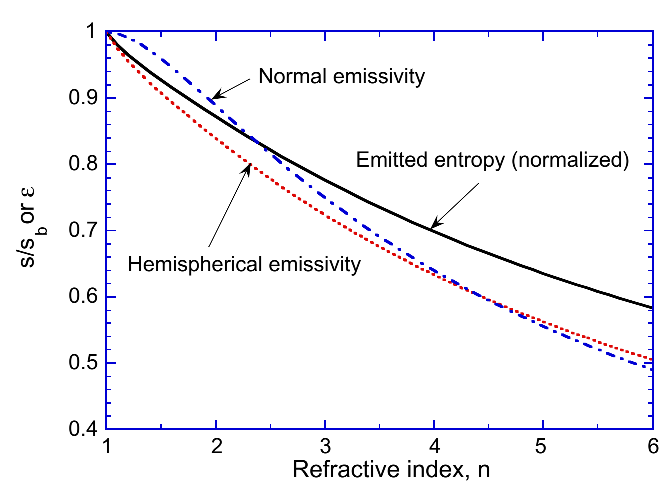

Fig. 6. Emitted entropy flux, normalized to that of a blackbody at the same temperature, hemispherical emissivity, and normal emissivity versus the refractive index of the emitting medium.

Table 1
Entropy flux for a free-emitting semi-infinite medium

Refractive index (n)	1	2	3	4	5	6
Hemispherical emissivity	1	0.839	0.724	0.633	0.562	0.505
s/s_b (exact solution)	1	0.872	0.776	0.698	0.635	0.583
s/s_b (diffuse assumption)	1	0.874	0.781	0.705	0.643	0.592
Relative error	0	0.2%	0.6%	1.0%	1.2%	1.5%

evaluate the entropy intensity. The entropy intensity is then integrated over the hemisphere and wavelength and then the two polarization components are added. While the surface is not diffuse, it is interesting to see how much error it would cause in the entropy flux when the surface is assumed to be a diffuse surface with an emissivity equal to the hemispherical emissivity. Table 1 compares the entropy fluxes. Regardless of the large differences in the monochromatic temperature of the emitted radiation, the diffuse assumption gives excellent prediction for the entropy flux, which is less than 1% when the emissivity is higher than 0.65% and only 1.5% when the emissivity is 0.5.

3.3. Reflection and transmission of solar radiation by a window

Attention is now turned to the case of entropy generation for solar radiation at a glass window. The typical refractive index of fused silica is $n = 1.5$, and absorption can be neglected in the most important solar spectrum from about 0.25 μm to 3.5 μm. The transmittance and reflectance can be calculated based on the ray-tracing method so that the transmitted and reflected intensities can be evaluated for each polarization as functions of the incidence polar angle [27]. The incident, reflected, and transmitted entropy intensities can be evaluated based on the spectral energy intensities. Because the radiation from the sun is confined in a small solid angle, it can be considered as a nearly collimated beam. In the calculation, the temperature of the sun is assumed to be $T_0 = 5800$ K. For illustration purpose, atmospheric absorption and scattering are neglected so that the intensity arriving at the window is taken to be the same as that of a blackbody at T_0. The sum of the reflected and transmitted entropy fluxes will be greater than the incident entropy flux due to irreversibility. The difference is the entropy generation.

The nondimensionalized total and spectral entropy generation is shown in Fig. 7, where q_0 is the incident heat flux and is equal to the blackbody emissive power of the sun since scattering and absorption by the atmosphere is neglected. In reality, atmospheric effects will not only reduce the incoming intensity of the solar radiation but also its monochromatic temperature. The curves are plot-

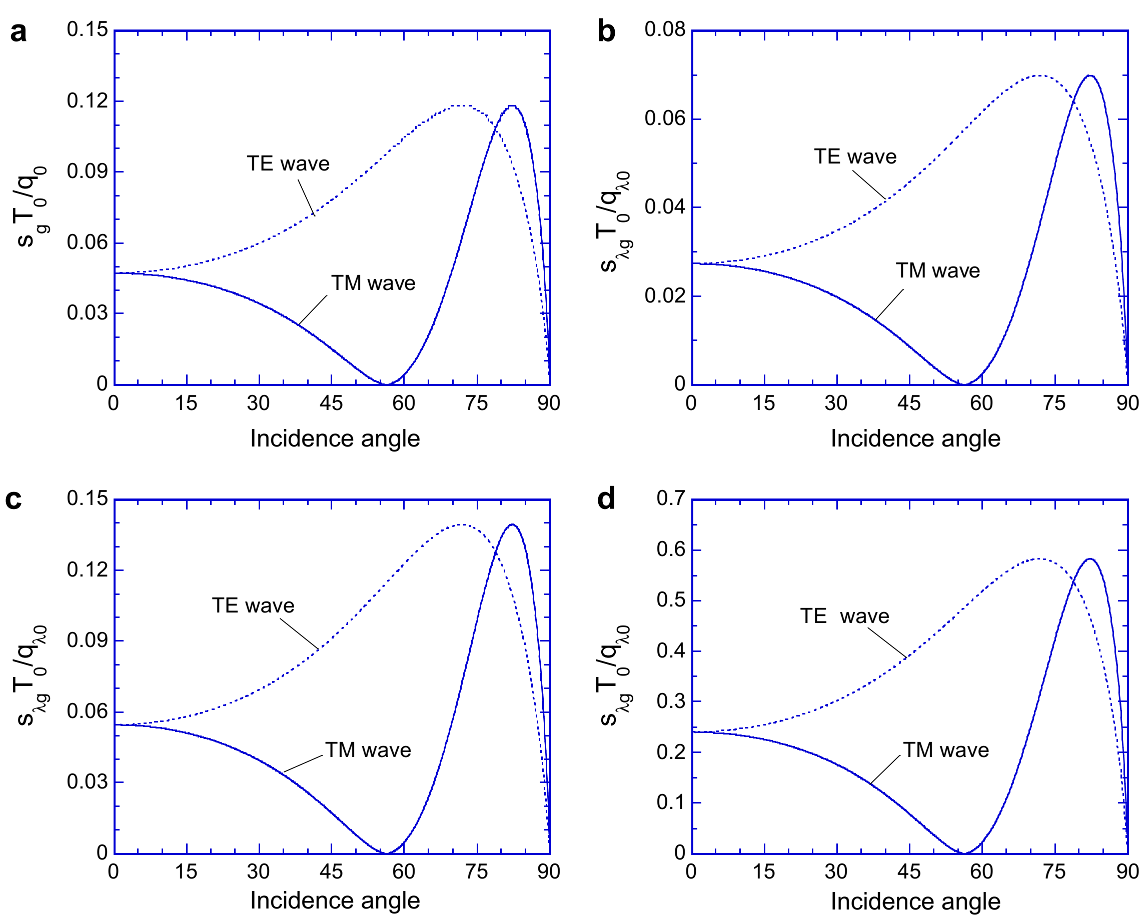

Fig. 7. Total and spectral entropy generation of solar radiation upon reflection and transmission through a glass window, where T_0 is the temperature of the sun, $q_0 = \sigma T_0^4$, and $q_{\lambda 0} = e_{\lambda,b}(\lambda, T_0)$. (a) Total; (b) $\lambda = 0.25$ μm; (c) $\lambda = 0.5$ μm; (d) $\lambda = 2.5$ μm.

ted for both TE wave and TM wave. For TE wave, the reflectance increases as the incidence angle increases. At the glazing angle, all the incident radiation is reflected and the entropy generation becomes zero for both polarizations. For TM wave, the reflectance is first reduced until the Brewster angle, which is 56.3° with $n = 1.5$. At the Brewster angle, all incident radiation is transmitted and the entropy generation is zero. The peak entropy generation corresponds to the case when the incident power is split nearly equally into the transmitted and reflected beams. The angular dependence of the spectral entropy generation follows the same trend for corresponding polarization. However, the entropy generation normalized to the spectral intensity increases rapidly as the wavelength increases. Not surprisingly, the nondimensional total entropy generation is close to the spectral entropy generation at the wavelength (0.5 μm) close to the maximum wavelength of emission.

3.4. Radiative transfer between parallel plates

So far, the discussion about free emission, reflection, and transmission may be viewed as a natural extension of the more complicated thermodynamic models of photon radiation, as summarized by Landsberg and Tonge [16] in 1980. The final example is for two large parallel plates at temperatures T_1 and T_2, separated by vacuum, as shown in Fig. 8. For convenience of discussion without loss of generality, it is assumed that $T_1 \geqslant T_2$. The surfaces of the plates are assumed diffuse and gray with emissivities ε_1 and ε_2, respectively. The separation distance is sufficiently large so that the near-field effects can be neglected [4]. It is quite surprising that a proper entropy analysis of such a basic radiative heat transfer problem has to wait until now.

The condition that both surfaces are diffuse and gray allows the determination of the forward intensity I_λ^+ and backward intensity I_λ^- as follows:

$$I_\lambda^+ = \frac{\varepsilon_1 I_{\lambda,\mathrm{b1}} + (1-\varepsilon_1)\varepsilon_2 I_{\lambda,\mathrm{b2}}}{1-(1-\varepsilon_1)(1-\varepsilon_2)} \tag{17}$$

and

$$I_\lambda^- = \frac{\varepsilon_1(1-\varepsilon_2) I_{\lambda,\mathrm{b1}} + \varepsilon_2 I_{\lambda,\mathrm{b2}}}{1-(1-\varepsilon_1)(1-\varepsilon_2)} \tag{18}$$

where $I_{\lambda,\mathrm{b1}}$ and $I_{\lambda,\mathrm{b2}}$ are Planck's distributions evaluated at T_1 and T_2, respectively. The radiation can be considered unpolarized because of the diffuse-gray assumption. Eq. (18) can be obtained using the ray-tracing method [27] as shown in Fig. 8. The forward and backward intensities can be substituted into Eq. (5) to calculate the monochromatic temperatures: T_λ^+ and T_λ^-, respectively, for the forward and backward radiation. In the special case when $\varepsilon_1 = 0$ but $\varepsilon_2 \neq 0$, $I_\lambda^+ = I_\lambda^- = I_{\lambda,\mathrm{b2}}$. The photon gas will be in equilibrium with surface 2. On the other hand, if surface 2 is perfectly reflecting, then the photon gas will be in equilibrium with surface 1. When $\varepsilon_1 = \varepsilon_2 = 1$, i.e., both surfaces are blackbodies, $T_\lambda^+ = T_1$ and $T_\lambda^- = T_2$, the forward stream and backward stream of photons can be viewed as being at different equilibrium states. In the extreme case when $T_1 = T_2$, it can be seen from Eq. (18) that $I_\lambda^+ = I_\lambda^- = I_{\lambda,\mathrm{b1}} = I_{\lambda,\mathrm{b2}}$, suggesting that a complete or *stable equilibrium state* [23] will be established. When nonideal surfaces are involved, the monochromatic temperature will be wavelength dependent, as can be seen from Fig. 9 for $T_1 = 1500$ K, $T_2 = 300$ K. In general $T_1 \geqslant T_\lambda^+ \geqslant T_\lambda^- \geqslant T_2$. In the case when $\varepsilon_2 = 0$, the monochromatic temperature is T_1. When $\varepsilon_1 = 0.2$ and $\varepsilon_2 = 1$, $T_\lambda^- = T_2$ but T_λ^+ is wavelength dependent. When $\varepsilon_1 = \varepsilon_2 = 0.5$, both T_λ^+ and T_λ^- decrease towards longer wavelengths.

The strategy of computing the entropy is to evaluate the entropy intensities using Eq. (2) by substituting the forward and backward intensities calculated from Eq. (18). The results give L_λ^+ and L_λ^- that are independent of the polar angle. Hence, the entropy fluxes can be calculated by

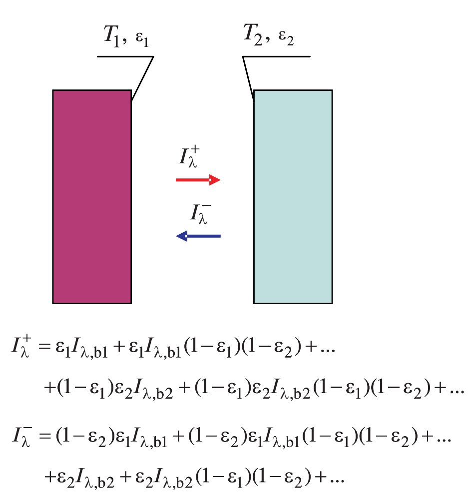

Fig. 8. Radiative heat transfer between two plates, showing the ray-tracing scheme for the forward and backward intensities, assuming $T_1 \geqslant T_2$.

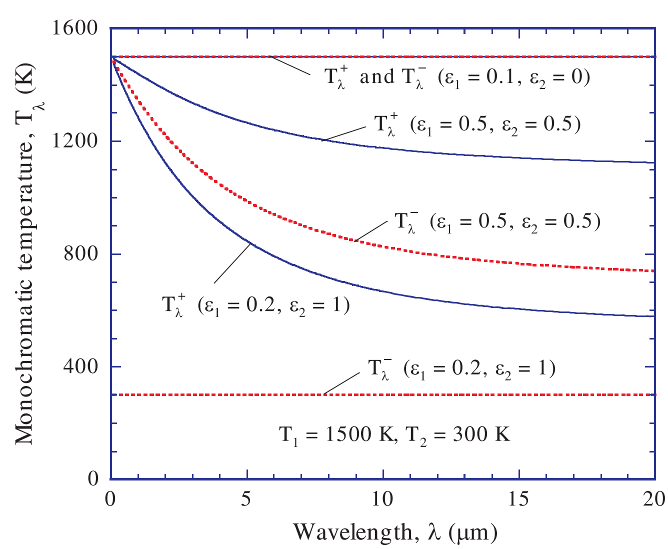

Fig. 9. Monochromatic temperature versus wavelength when $T_1 = 1500$ K and $T_2 = 300$ K with different emissivity combinations.

$$s^+ = \pi \int_0^\infty L_\lambda^+ \, d\lambda \quad \text{and} \quad s^- = \pi \int_0^\infty L_\lambda^- \, d\lambda \tag{19}$$

Note that for surface 1, the "+" sign is for the outgoing and the " − " sign is for the incoming, and the opposite is the case for surface 2. The entropy generation at each surface due to radiative heat transfer can thus be evaluated using Eq. (10). Let $q_{12} = q^+ - q^-$ and $s_{12} = s^+ - s^-$, which are the net heat transfer and entropy transfer, the entropy generation at each surface can be expressed as

$$s_{g,1} = s_{12} - \frac{q_{12}}{T_1} \geqslant 0 \quad \text{and} \quad s_{g,2} = \frac{q_{12}}{T_2} - s_{12} \geqslant 0 \tag{20}$$

The total entropy generation per unit heat transfer is: $(s_{g,1} + s_{g,2})/q_{12} = 1/T_2 - 1/T_1$, which is independent of the emissivity of any surface. The difference between radiation and conduction (or diffusion) heat transfer between two constant-temperature objects is that, in conduction, entropy generation occurs inside the medium (presumably the boundary resistance is negligible). In radiation, on the contrary, entropy generation occurs at the interfaces. The emissivities affect the fraction of entropy generated by individual surfaces, as shown in Fig. 10a, where $s_{g,1}/(s_{g,1} + s_{g,2})$ and $s_{g,2}/(s_{g,1} + s_{g,2})$ are plotted in percentage. When both surfaces are black, because $q_{12} = \sigma T_1^4 - \sigma T_2^4$ and $s_{12} = \frac{4}{3}\sigma T_1^3 - \frac{4}{3}\sigma T_2^3$, it can easily be verified that 8.1% entropy generation is at surface 1. However, the fraction of entropy generation at surface 1 increases as its emissivity decreases. Assuming surface 2 is black, then $q_{12} = \varepsilon_1 \sigma (T_1^4 - T_2^4)$, if s_{12} were also scaled with ε_1, that is $s_{12} = \frac{4}{3}\varepsilon_1 \sigma (T_1^3 - T_2^3)$, the fraction of entropy generation would not change with ε_1 at all. The reason for the redistribution of entropy generation is explained next.

The emitted entropy intensities for surfaces 1 and 2 can be obtained from Eq. (12) with

$$X_1 = \frac{\varepsilon_1 I_{\lambda,b1}}{I_\lambda^+} \quad \text{and} \quad X_2 = \frac{\varepsilon_2 I_{\lambda,b2}}{I_\lambda^-} \tag{21}$$

respectively. The emitted total entropy flux can be evaluated using $s_{emit} = \pi \int_0^\infty L_{\lambda,emit} \, d\lambda$ for each surface under the diffuse assumption. Fig. 10b shows the emitted entropy normalized by $\frac{4}{3}\varepsilon\sigma T^3$ for the corresponding surface. It is clear that $\frac{4}{3}\varepsilon\sigma T^3$ does not represent the emitted entropy for either surface. What is more interesting is that the emitted entropy by surface 1 is always greater than (or at least equal to) $\frac{4}{3}\varepsilon_1\sigma T_1^3$, whereas the emitted entropy by surface 2 is always smaller than (or at most equal to) $\frac{4}{3}\varepsilon_2\sigma T_2^3$. Note that the temperature of surface 2 is much lower than that of surface 1 in the numerical example, resulting in a backward flux usually much smaller than the forward flux. When surface 2 is a blackbody, the emission from surface 1 is close to free emission, and the entropy of emission is greater than that would be predicted by $\frac{4}{3}\varepsilon_1\sigma T_1^3$, because the emitted photons do not follow an equilibrium distribution. The increase of the entropy emitted by surface 1 with decreasing ε_1 causes an increase in the net entropy transfer between the two surfaces per unit heat transfer: s_{12}/q_{12}.

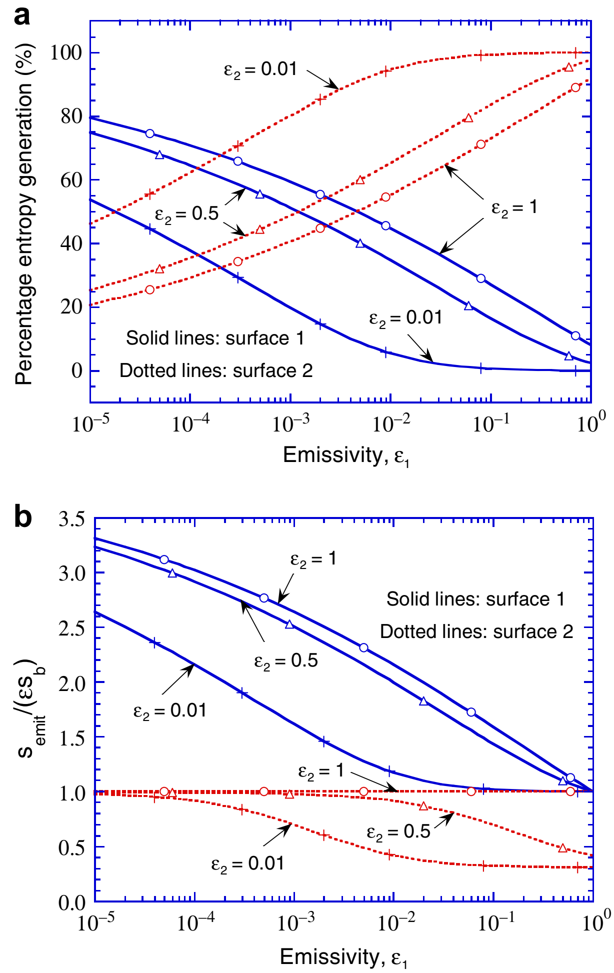

Fig. 10. (a) Percentage entropy generation and (b) the emitted entropy by each surface for $T_1 = 1500$ K and $T_2 = 300$ K. The emitted entropy is normalized to the product of the emissivity and the entropy emitted by a blackbody at the surface temperature.

According to Eq. (20), $s_{g,1}/q_{12}$ will increase and $s_{g,2}/q_{12}$ will decrease.

When the emissivity of surface 2 is reduced, a large amount of photons will be reflected back towards surface 1, resulting in an increase of I_λ^+ and a reduction of the entropy associated with the emitted photons with respect to $\frac{4}{3}\varepsilon_1\sigma T_1^3$. At the same time, the reflection increases I_λ^- and subsequently the monochromatic temperature T_λ^-. While the emitted number of photons by surface 2 does not change, the total entropy emitted by surface 2 is reduced. Lowering the $s_{emit,1}/(\varepsilon_1 s_{b1})$ has more significant effect in reducing s_{12}/q_{12}. Hence, as ε_2 decreases, for the same ε_1, the fraction of entropy generation by surface 1 decreases and the fraction of entropy generation by surface 2 increases. When one surface is highly reflecting, the photon gas is close to the equilibrium state of the other surface; hence, most of the entropy generation occurs at the highly reflecting surface.

To date, the procedure mentioned above seems to be the only plausible method for the determination of entropy generation and emission by individual surfaces in one of the simplest radiative heat transfer problems. In a direct energy conversion device, the photon energy from a high-temperature source in certain frequency region will be absorbed and converted into electricity rather than thermal energy. It is important to take into account the spectral dependence of the radiative properties of both the emitter and absorber, considering multiple reflections and quantum efficiency of the device. The method presented above should enable such an analysis to be made properly based on the principles of thermodynamics and the physics of thermal radiation.

4. Conclusions

A systematic method is developed in the present work for entropy analysis of radiative heat transfer between surfaces. Expressions that are consistent with nonequilibrium thermodynamics have been derived rigorously under the three hypotheses. The concept of partial thermodynamic equilibrium is utilized to provide a physical interpretation of the monochromatic radiation temperature under nonequilibrium radiation environment. The key to evaluate radiation entropy and temperature is to calculate these quantities according to the combined intensity in each wavelength and direction. Sometimes it may even be necessary to evaluate them separately for each polarization. The fraction of entropy carried by each individual ray is the same as the fraction of energy intensity or photon numbers in that ray.

Along with presenting some interesting results, the present paper has also clarified some confusions and unjustifiable approximate expressions in the literature. Until now, no theories exist for proper evaluation of the emitted and generated entropies by individual surfaces during radiative heat transfer processes. The method presented here has been successfully applied to the evaluation of the entropies emitted and generated at each surface in the radiative heat transfer problem between two diffuse-gray plates. The procedure developed in the present paper can also be applied to perform second-law analysis of industrial systems involving thermal radiative heat transfer, by taking into account the spectral nature of thermal radiation, multiple reflections, polarization, and spectral radiative properties.

At present, a satisfactory second-law interpretation of the near-field radiation does not exist. Because of the rapid advancement of nanoengineering and the increasing awareness of energy related issues, the study of thermodynamics of near-field radiation is expected to be an important research area that will greatly impact future development of micro/nanoscale energy conversion technologies.

Acknowledgements

This work was supported by the National Science Foundation (CTS-0327117 and CTS-0500113). The authors thank Keunhan Park for valuable discussions and Bong Jae Lee for his assistance with the calculation.

References

[1] T.J. Coutts, A review of progress in thermophotovoltaic generation of electricity, Renew. Sust. Energy Rev. 3 (1999) 77–184.

[2] A. Narayanaswamy, G. Chen, Surface modes for near field thermophotovoltaics, Appl. Phys. Lett. 82 (2003) 3544–3546.

[3] I. Celanovic, F. O'Sullivan, M. Ilak, J. Kassakian, D. Perreault, Design and optimization of one-dimensional photonic crystals for thermophotovoltaic applications, Opt. Lett. 29 (2004) 863–865.

[4] C.J. Fu, Z.M. Zhang, Nanoscale radiation heat transfer for silicon at different doping levels, Int. J. Heat Mass Transfer 49 (2006) 1703–1718.

[5] A. Bejan, Entropy Generation Minimization, CRC Press, Boca Raton, FL, 1996.

[6] M. Planck, On the law of distribution of energy in the normal spectrum, Annalen der Physik 4 (1901) 553–563.

[7] G.P. Beretta, E.P. Gyftopoulos, Electromagnetic radiation: a carrier of energy and entropy, ASME Winter Annual Meeting, Dallas, TX, AES-Vol. 19, November 1990.

[8] C. Essex, D.C. Kennedy, R.S. Berry, How hot is radiation? Am. J. Phys. 71 (2003) 969–978.

[9] R. Petela, Exergy of heat radiation, J. Heat Transfer 86 (1964) 187–192.

[10] R. Petela, Exergy of undiluted thermal radiation, Solar Energy 74 (2003) 469–488.

[11] S.M. Jeter, Maximum conversion efficiency for the utilization of direct solar radiation, Solar Energy 26 (1981) 231–236.

[12] A. Gribik, J.F. Osterle, The second law efficiency of solar energy conversion, J. Solar Energy Eng. 106 (1984) 16–21.

[13] A. Bejan, Advanced Engineering Thermodynamics, second ed., Wiley, New York, 1997 (Chapter 9).

[14] V.S. Arpaci, Radiation entropy production-heat lost to entropy, Adv. Heat Transfer 21 (1991) 239–276.

[15] P.T. Landsberg, G. Tonge, Thermodynamics of the conversion of diluted radiation, J. Phys. A 12 (1979) 551–561.

[16] P.T. Landsberg, G. Tonge, Thermodynamic energy conversion efficiencies, J. Appl. Phys. 51 (1980) R1–R20.

[17] S.E. Wright, D.S. Scott, J.B. Haddow, M.A. Rosen, On the entropy of radiative transfer in engineering thermodynamics, Int. J. Eng. Sci. 39 (2001) 1691–1706.

[18] M.D. Whale, Effective flux temperature formulation for energy conversion using microscale thermal radiation, International Mechanical Engineering Congress and Exposition, New York, November 2001, Paper No. HTD-24275.

[19] M. Caldas, V. Semiao, Entropy generation through radiative transfer in participating media: analysis and numerical computation, J. Quant. Spectrosc. Radiat. Transfer 96 (2005) 423–437.

[20] L.H. Liu, S.X. Chu, On the entropy generation formula of radiation heat transfer processes, J. Heat Transfer 128 (2006) 504–506.

[21] M.F. Modest, Radiative Heat Transfer, second ed., Academic Press, San Diego, CA, 2003.

[22] M. Planck, The Theory of Heat Radiation, Dover Publications, New York, 1959.

[23] E.P. Gyftopoulos, G.P. Beretta, Thermodynamics: Foundations and Applications, Macmillan, New York, 1991, also Dover Publisher, New York, 2005.

[24] Z.M. Zhang, Surface temperature measurement using optical techniques, Ann. Rev. Heat Transfer 11 (2000) 351–411.

[25] C.E. Mungan, Radiation thermodynamics with application to lasing and fluorescent cooling, Am. J. Phys. 73 (2005) 315–322.

[26] L. Mandel, E. Wolf, Optical Coherence and Quantum Optics, Cambridge University Press, Cambridge, UK, 2005.

[27] R. Siegel, J.R. Howell, Thermal Radiation Heat Transfer, fourth ed., Taylor and Francis, New York, 2002.

[28] Q.Z. Zhu, Z.M. Zhang, Anisotropic slope distribution and bidirectional reflectance of a rough silicon surface, J. Heat Transfer 126 (2004) 985–993.